

# Upregulated *BLM* and *RECQL4* in Osteosarcoma: Association with Poor Prognosis, Immune Cell Infiltration, and Inhibitory Effects of Sphingosine Kinase I Inhibitor II/Pilaralisib

Jv Chen<sup>1,\*</sup>, Yongli Situ<sup>2,\*</sup>, Jie Cai<sup>1</sup>, Wenyu Liao<sup>1</sup>, Dongbo Jiang<sup>1</sup>, Chengshuo Huang<sup>2</sup>, Jinchang Zheng<sup>2</sup>, Lijiao Peng<sup>3</sup>, Hao Lin<sup>2</sup>

<sup>1</sup>Department of Pharmacy, Affiliated Hospital of Guangdong Medical University, Zhanjiang, Guangdong, 524002, People's Republic of China;

<sup>2</sup>Orthopedic Center, Affiliated Hospital of Guangdong Medical University, Zhanjiang, Guangdong, 524002, People's Republic of China; <sup>3</sup>Department of Digestive System Oncology, Oncology Hospital, Affiliated Hospital of Guangdong Medical University, Zhanjiang, Guangdong, 524002, People's Republic of China

\*These authors contributed equally to this work

Correspondence: Hao Lin, Orthopedic Center, Affiliated Hospital of Guangdong Medical University, No. 57 Renmin Avenue South, Zhanjiang, Guangdong, 524002, People's Republic of China, Email [linhao@gdmu.edu.cn](mailto:linhao@gdmu.edu.cn); Lijiao Peng, Department of Digestive System Oncology, Oncology Hospital, Affiliated Hospital of Guangdong Medical University, No. 57 Renmin Avenue South, Zhanjiang, Guangdong, 524002, People's Republic of China, Email [244348566@qq.com](mailto:244348566@qq.com)

**Purpose:** *BLM* and *RECQL4*, key RecQ helicases and “genome guardians”, maintain genomic stability. Their abnormal function/dysregulated expression is linked to tumorigenesis, but their roles in osteosarcoma (OS) remain unclear.

**Patients and Methods:** Comprehensive bioinformatic analyses (multiple public databases) assess OS-related expression, gene networks, prognosis, targets, and drugs. Cellular experiments verified the effects of these compounds on 143B cell proliferation, migration, and invasion.

**Results:** *BLM* and *RECQL4* were significantly upregulated in OS tissues compared to normal tissues, correlating with a poor prognosis. Among the 153 patients with OS, 9% and 7% had altered *BLM* and *RECQL4* expression, respectively. Abnormal methylation of *BLM* and *RECQL4* may affect OS. *BLM*, *RECQL4*, and their altered neighboring genes (ANGs) form interaction networks that regulate tumor metabolism, proliferation, migration, and apoptosis. Their miRNA and kinase targets in OS were also identified. *BLM* and *RECQL4* expression was negatively correlated with OS immune cell infiltration. In addition, anti-PD-1/CTLA-4/PD-L1 therapy, Sphingosine kinase 1 inhibitor II, and pilaralisib inhibited OS cell viability (by downregulating *BLM* or *RECQL4*) and the proliferation, migration, and invasion of 143B cells. Knockdown of *BLM* or *RECQL4* suppressed the migration and invasion of 143B cells.

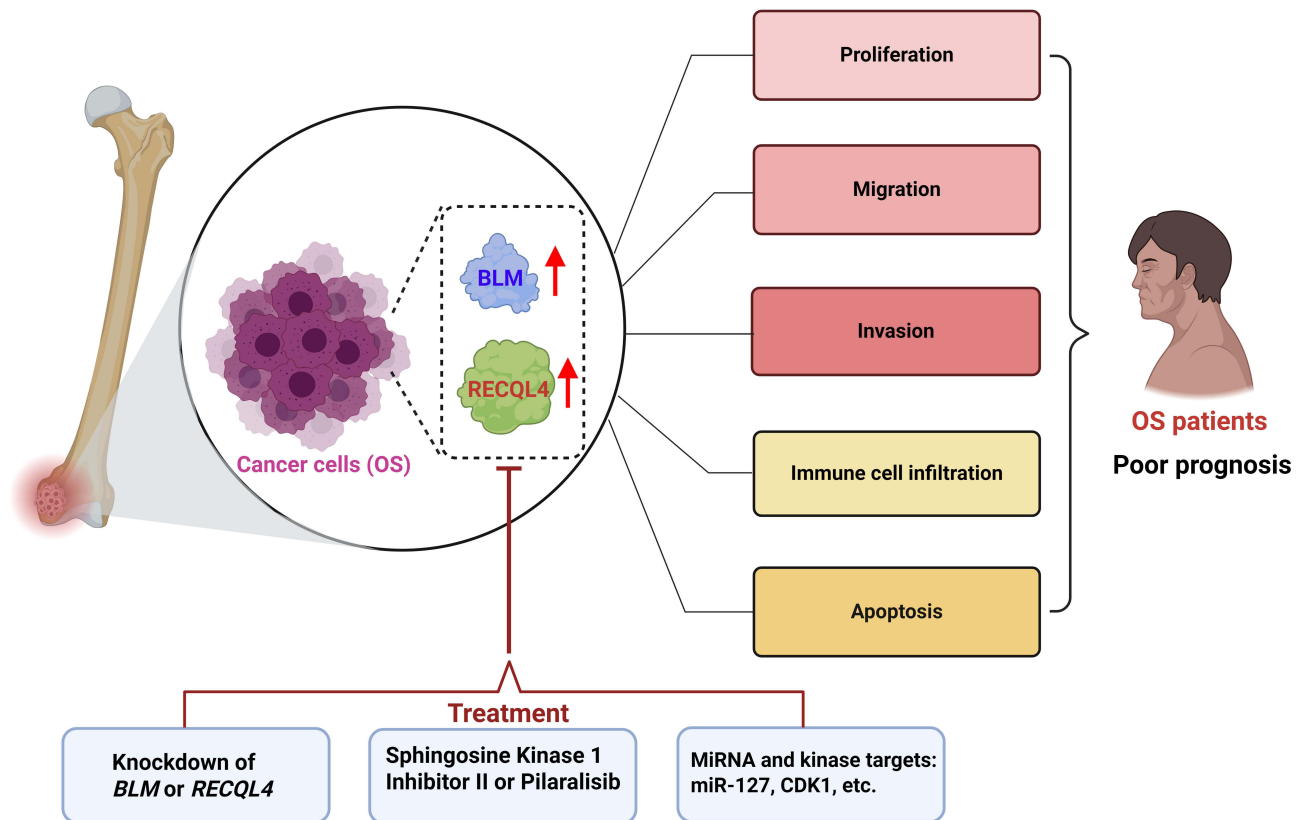
**Conclusion:** *BLM* and *RECQL4* are promising prognostic biomarkers and therapeutic targets for OS.

**Keywords:** *BLM*, *RECQL4*, osteosarcoma, gene regulatory network, immunotherapy, prognosis, biomarker, bioinformatics

## Introduction

Osteosarcoma (OS) is the most common primary malignant bone tumor, accounting for approximately 56% of all malignant bone tumors, and predominantly affects children and adolescents.<sup>1,2</sup> Currently, the standard treatment regimen of neoadjuvant chemotherapy–consolidation chemotherapy has achieved remarkable outcomes in patients with localized OS,<sup>3</sup> and the annual survival rate has stabilized at 60%–70%.<sup>4</sup> However, OS exhibits a strong tendency for local infiltration and early metastasis, particularly when metastasis to the pulmonary parenchyma is preferred. According to statistics, 30–50% of patients will experience recurrence,<sup>5</sup> and 15–20% of newly diagnosed patients with OS will develop metastasis,<sup>6</sup> with a 5-year survival rate of only 20–30%.<sup>7</sup> The problems associated with high disability and mortality rates

## Graphical Abstract



in OS remain unresolved. Traditional treatment methods, such as surgery, chemotherapy, and radiotherapy, face numerous challenges when dealing with metastatic and recurrent OS.<sup>8</sup> Targeted therapy for OS mainly focuses on anti-angiogenic small-molecule inhibitors (such as regorafenib and sorafenib).<sup>9</sup> Although these drugs have a certain therapeutic effect on metastatic OS, the progression-free survival of patients is short, and the objective response rate is low.<sup>10</sup> Phenomena such as chemoresistance and tumor immune escape often occur during treatment and are largely driven by cancer stem cells and the tumor microenvironment.<sup>11,12</sup> The pathogenesis of OS is multifactorial, involving a convergence of genetic, immune, and environmental factors.<sup>13–15</sup> Therefore, innovative treatment strategies are urgently needed to improve the overall survival rates of patients with OS. Of note, aberrant alterations in the OS expression profile are expected to offer promising avenues for identifying anti-OS biomarkers and developing novel therapeutic strategies.<sup>16–19</sup>

The RecQ helicase family comprises highly conserved helicases that have evolved and are crucial for maintaining genomic stability.<sup>20</sup> The human RecQ family comprises five proteins: *RECQL*, *BLM*, *WRN*, *RECQL4*, and *RECQL5*.<sup>20</sup> RecQ helicases use energy from ATP hydrolysis to unwind double-stranded DNA and are involved in metabolic processes such as DNA recombination, replication, and repair.<sup>21</sup> *BLM* and *RECQL4* are associated with the occurrence, development, and prognosis of various tumors. *BLM* is located at 15q26.1 on the chromosome, and its mutation is associated with human cancers.<sup>22</sup> *BLM* plays a key role in the development of various cancers. In breast cancer, the overexpression of *BLM* mRNA and protein has significant prognostic value, and an increase in its expression is associated with reduced distant metastasis-free survival in patients.<sup>23</sup> In lung adenocarcinoma, patients with low *BLM* expression have a higher overall survival rate, and the frequency of *BLM* mutations is higher in male than in female patients.<sup>24</sup> *BLM* expression is upregulated in prostate cancer cells, and *BLM* inhibition reduces cell proliferation and

promotes apoptosis.<sup>25</sup> *RECQL4* is located on chromosome 8q24.3, and patients carrying pathogenic variants are more prone to developing OS.<sup>26</sup> Abnormal *RECQL4* expression affects the prognosis of various cancers. In hematological malignancies, such as acute myeloid leukemia in patients with abnormal karyotypes, low expression of *RECQL4* and *BLM* is associated with poor outcomes, whereas overexpression of *RECQL4* indicates a better prognosis.<sup>27</sup> However, significant knowledge gaps remain regarding the roles of *BLM* and *RECQL4* in OS pathogenesis.

In this study, we comprehensively analyzed the expression patterns, gene regulatory networks, and prognostic prediction values of *BLM* and *RECQL4* in patients with OS using systematic bioinformatics analysis and in-depth cellular experiments. Additionally, we explored potential target sites and possible therapeutic drugs. This study revealed the intrinsic connections between OS, *BLM*, and *RECQL4* and successfully screened novel potential targets and candidate drugs for OS treatment. This study provides an important theoretical basis and data support for further exploration of the pathogenesis of OS and the development of innovative treatment strategies, and is expected to bring new breakthroughs in improving the clinical prognosis of patients with OS.

## Materials and Methods

### GEPIA

We used GEPIA (<http://gepia.cancer-pku.cn/index.html>) to analyze the relationship between *BLM* and *RECQL4* expression and OS. The screening criteria were as follows: (1) genes: *BLM* and *RECQL4*; (2) dataset: OS; and (3) 262 patients; threshold-setting conditions: *P*-value cutoff = 0.05. We used the Student's *t*-test to analyze the expression of *BLM* and *RECQL4* in OS. The Kaplan–Meier curve was used to analyze the prognosis of patients with OS.<sup>28</sup> The data used for analysis were acquired between March 2025 and May 2025.

### Biomarker Exploration of Solid Tumors (BEST)

We used BEST ([https://rookieutopia.com/app\\_direct/BEST/](https://rookieutopia.com/app_direct/BEST/)) to analyze protein expression, immune cell infiltration, candidate agents, and immunotherapy targeting *BLM* and *RECQL4* in OS. The “Cell infiltration”, “Immunotherapy”, and “Candidate agents” modules of the BEST database were used to analyze the Gene Expression Omnibus and TCGA gene expression data using the following screening criteria: (1) genes: *BLM* and *RECQL4*; (2) dataset: OS (15 datasets and 1714 patients).<sup>28</sup>

### MethSurv

We used MethSurv (<https://biit.cs.ut.ee/methsurv/>), a specialized bioinformatics tool, to comprehensively analyze DNA methylation profiles and their associations with prognosis at the genomic loci of *BLM* and *RECQL4* in patients with OS.<sup>29</sup>

### scRNA-Seq Data Analysis

The scRNA-seq data of OS tissues were obtained from the GEO scRNA-seq dataset (GSE162454) deposited in the public Tumor Immune Single-cell Hub (TISCH) database (<http://tisch.compgenomics.org/home/>).<sup>30</sup> The values in the single-cell -level expression matrix were normalized using the NormalizeData method in “Seurat” to scale the raw counts (UMI) in each cell to 10,000. A uniform analysis algorithm (MAESTRO) was used for quality control, clustering, and cell-type annotation across datasets. The GSE162454 dataset contains 46,544 cells from six OS tissue samples. scRNA-seq was performed using the 10× Genomics platform.

### cBioPortal

We used cBioPortal (<http://cbioportal.org>) to analyze alterations in *BLM* and *RECQL4* expression. A total of 153 OS samples were analyzed, and z-scores for mRNA expression relative to all samples (log RNA Seq V2 RSEM) were obtained using a z-score threshold of  $\pm 2.0$ .<sup>28</sup>

## STRING and GeneMANIA

STRING (<https://string-db.org/cgi/input.pl>) was used to build a low-confidence (0.150) PPI network and screen for the human species. GeneMANIA (<http://www.genemania.org>) was used to explore the functions of *BLM*, *RECQL4*, and the top 50 ANGs.<sup>28</sup>

## Metascape

Metascape (<https://metascape.org>) was used to analyze the functions and signaling pathways of *BLM*, *RECQL4*, and the top 50 ANGs.<sup>28</sup> The following were the threshold-setting conditions: *P*-value cutoff = 0.05, minimum enrichment score = 1.5, and minimum overlap = 3.

## LinkedOmics

LinkedOmics (<http://www.linkedomics.org/>) was used to identify kinase targets, miRNA targets, and differentially expressed genes related to *BLM* and *RECQL4*.<sup>28</sup> The screening criteria were as follows: (1) genes: *BLM* and *RECQL4*; (2) dataset: RNASeq (OS); and (3) 259 patients; the statistical test was selected as the Pearson correlation test.

## Timer

TIMER (<https://cistome.shinyapps.io/timer/>) was used to analyze the correlation between *BLM* and *RECQL4* expression and immune cell infiltration.<sup>28</sup> The screening criteria were as follows: (1) genes: *BLM* and *RECQL4*, and (2) dataset: OS.

## Genomics of Drug Sensitivity in Cancer Analysis

The Genomics of Drug Sensitivity in Cancer database (<http://www.cancerRxgene.org>) was used to identify drugs targeting *BLM* and *RECQL4* and to predict their anti-OS activity.<sup>28</sup> The screening criteria were as follows: (1) drugs: sphingosine kinase 1 inhibitor II and pilaralisib; (2) dataset: GDSC1; and (3) Tissue-specific analysis parameter: Pan-Cancer and OS.

## Cell Culture

143B cells, supplied by the National Collection of Authenticated and GEM Cell Cultures (China), were grown in Dulbecco's Modified Eagle's Medium (DMEM; Gibco, USA) containing 10% fetal bovine serum (Gibco) and 1% antibiotics (Gibco) at 37 °C with 5% CO<sub>2</sub>.

## Cell Viability Assay

The viability of 143B cells was evaluated using the Cell Counting Kit-8 (Biosharp, China), according to the manufacturer's instructions. Cells were seeded in 96-well plates and treated with sphingosine kinase 1 inhibitor II (MedChemExpress, USA) (5, 10, 20, 40, 80, 160, and 320 μM) and pilaralisib (MedChemExpress) (6.25, 12.5, 25, 50, 100, 200, and 400 μM) for 24 h. The absorbance of each well was measured at 450 nm using a microplate reader.

## Wound-Healing Scratch Assay (Cell Migration)

To evaluate the effects of sphingosine kinase 1 inhibitor II and pilaralisib on the adhesion and motility of 143B cells,  $2.5 \times 10^5$  cells were seeded in 6-well plates. When the cells reached confluence, a 100 μL pipette tip was used to gently scratch the cell monolayer to create four scratch areas. Subsequently, the cells were washed twice with PBS to remove non-adherent cells. The control, sphingosine kinase 1 inhibitor II (40 μM), and pilaralisib (50 μM) groups were established. Phase-contrast micrographs were captured immediately after scratching (0 h) and again at 24 h. Each group was assessed in at least three experiments.

## Transwell Assay (Invasion Assays)

For the Transwell assay, 143B cells ( $2 \times 10^4$ ) were resuspended in 200 μL DMEM and seeded into the upper well of 8-μm-pore chambers (Corning, USA) that had been coated with Matrigel (Corning). The control, sphingosine kinase 1

inhibitor II (40  $\mu$ M), and pilaralisib (50  $\mu$ M) groups were established. After incubation at 37 °C in 5% CO<sub>2</sub> for 36 h, the upper chamber was cleaned with a cotton swab, and the cells in the lower chamber were fixed with 4% paraformaldehyde, stained with 0.1% crystal violet, and washed three times with water. The number of cells per field was determined using a microscope (Nikon, Tokyo, Japan). Each group was assessed in at least three experiments.

## Immunofluorescence Microscopy

143B cells cultured in vitro and treated with sphingosine kinase 1 inhibitor II (40  $\mu$ M) and pilaralisib (50  $\mu$ M) were washed twice with PBS, fixed with 4% paraformaldehyde for 10 min at 26 °C, and washed twice with PBS for 5 min each. The membrane was permeabilized with 0.5% Triton X-100 for 10 min at 26 °C, then washed twice with PBS for 5 min each. This step was omitted if the protein was a membrane protein. After washing with PBS three times for 5 min each, the cells were blocked with 2% bovine serum albumin for 30 min at 26 °C and then incubated with BLM (1:100 dilution; Abcam, UK) and RECQL4 (1:100 dilution; Abcam) overnight at 4 °C. After three washes with PBS, the cells were incubated with the appropriate secondary antibody (Alexa Fluor 488; Beijing Solarbio Science & Technology Co., Ltd., China) for 30 min at 26 °C. After the slides were washed with PBS, 1  $\mu$ g/mL of nucleic acid dye DAPI (Beijing Solarbio Science & Technology Co., Ltd.) was added. Images were captured using an inverted fluorescence microscope (Nikon).

## Cell Transfection

To transiently suppress *BLM* and *RECQL4* expression, siRNAs (Ribo-Bio, China) were transfected into 143B cells using Lipofectamine 3000 (Shanghai Dafei Biotechnology Co., Ltd., China). All transfection procedures were performed according to the manufacturer's instructions. After transfecting the cells for 48 h, the transfection efficiency was tested using Western blotting analysis. Subsequently, we compared the migration and invasion of 143B cells before and after transfection, as described above.

## Western Blotting

Cellular proteins were extracted using radioimmunoprecipitation assay buffer (Beyotime). Next, 50  $\mu$ g of protein was subjected to a 12% sodium dodecyl sulfate–polyacrylamide gel electrophoresis. Polyvinylidene fluoride membranes were probed with antibodies against BLM (1:1000 dilution; Abcam, UK), RECQL4 (1:1000 dilution; Abcam, UK), and  $\beta$ -actin (1:1000 dilution; Abcam, UK). After developing the membrane with electrochemiluminescence reagent, the bands were imaged using a gel imaging system (Tanon, China).

## Statistical Analysis

Data from in vitro experiments are presented as mean  $\pm$  SD. An unpaired *t*-test or one-way analysis of variance was used accordingly. Statistical analyses were performed using GraphPad Prism 8. Statistical significance was set at  $P < 0.05$ .

## Results

### Expression and Prognosis of BLM and RECQL4 in OS

The transcript levels of *BLM* and *RECQL4* were significantly upregulated ( $P < 0.05$ ; [Figure 1A](#) and [B](#)) in patients with OS. *BLM* transcript levels were significantly lower in males than in females ( $P = 0.0017$ ; [Figure 1C](#)). However, *RECQL4* transcript levels were significantly higher in males than in females ( $P = 0.033$ ; [Figure 1D](#)). Furthermore, overall survival was longer in patients with OS who exhibited low *BLM* expression than in those with high *BLM* expression ( $P = 0.031$ ; [Figure 1E](#)). Disease-free survival was longer in patients with OS who had low *RECQL4* expression than in those with high *RECQL4* expression ( $P = 0.014$ ; [Figure 1F](#)).

### Genetic Alteration and DNA Methylation of BLM and RECQL4 in OS

We further assessed the genetic alterations in *BLM* and *RECQL4* in 153 patients with OS using data from the TCGA database. We found that *BLM* and *RECQL4* were altered by 9% and 7%, respectively, in patients with OS, with genetic

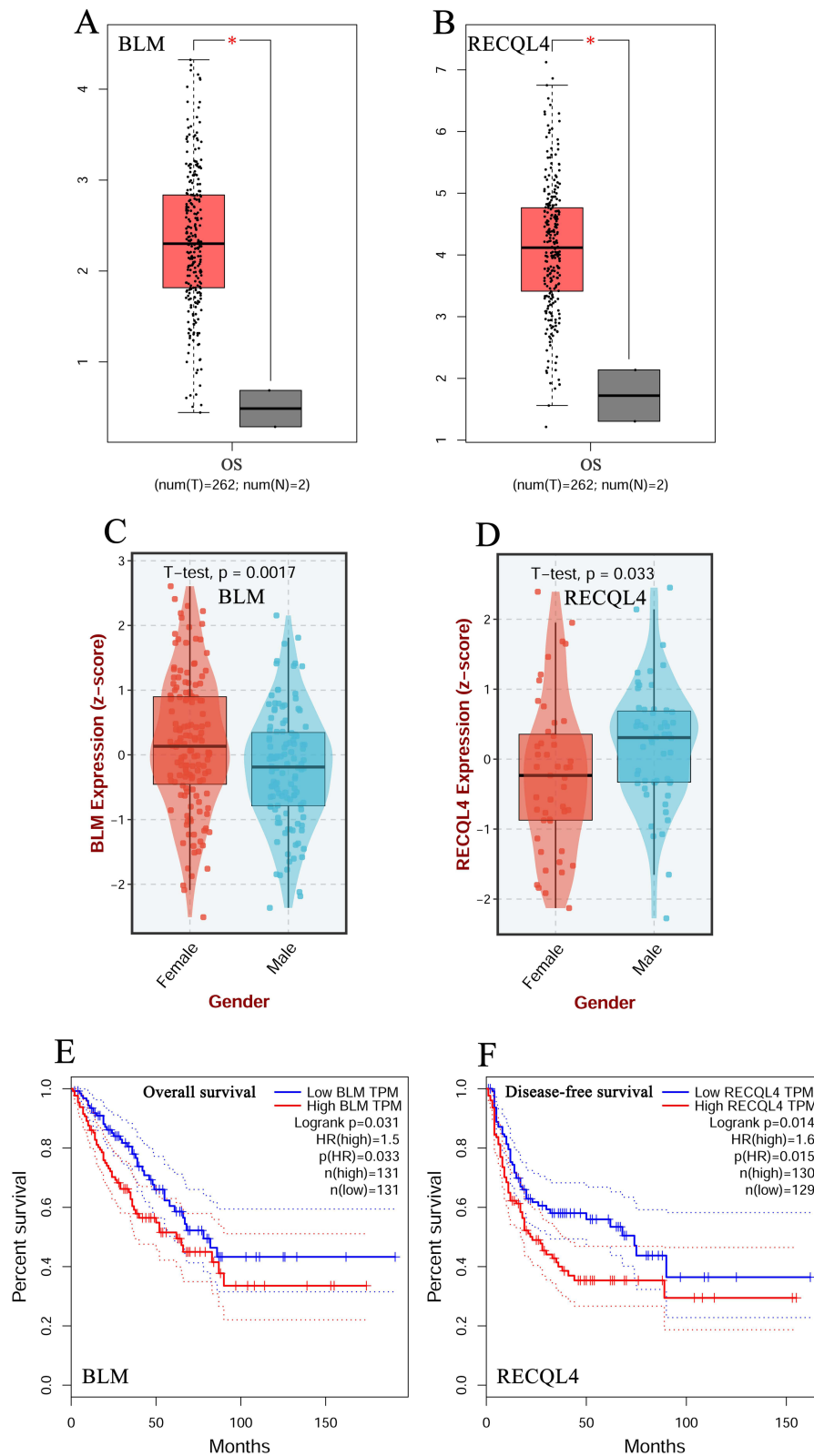


**Figure 1** Transcription levels and prognostic value of *BLM* and *RECQL4* in OS. (**A** and **B**) Transcription levels of *BLM* and *RECQL4* in patients with OS, respectively (GEPIA); (**C** and **D**) Transcription levels of *BLM* and *RECQL4* in patients with OS based on sex, respectively (BEST); (**E**) Overall survival curve of *BLM* in patients with OS (GEPIA); (**F**) Disease-free survival curve of *RECQL4* in patients with OS (GEPIA); \**P* < 0.05.

alterations primarily including amplification, high RNA levels, and low RNA levels ([Supplementary Figure 1A](#) and [B](#)). Next, we assessed the DNA methylation levels of *BLM* and *RECQL4* in patients with OS using the MethSurv tool. The DNA methylation levels of *BLM* significantly decreased at some CpG sites (cg06034771, cg19562400, cg08367959, cg11429664, cg19818642, cg02984193, cg25857018, cg02756768, cg25653141, cg01994513, and cg22690576;  $P < 0.05$ ; [Supplementary Figure 1C](#)) and significantly increased at others (cg13108397, cg26844732, cg01321816, and cg13410000) ( $P < 0.05$ ; [Supplementary Figure 1C](#)). Among the 15 predicted CpG sites of *BLM*, cg06034771, cg02756768, cg19818642, cg13108397, and cg02984193 were significantly correlated with OS ([Supplementary Figure 1D–H](#) and [Supplementary Table 1](#)). Patients with high *BLM* methylation at these CpG sites (cg06034771, cg02756768, cg19818642, and cg02984193) had better overall survival than those with low *BLM* methylation ([Supplementary Figure 1D–G](#)). However, patients with low *BLM* methylation at the CpG site (cg13108397) had better overall survival than those with high *BLM* methylation levels ([Supplementary Figure 1H](#)). Furthermore, *RECQL4* showed significantly increased DNA methylation levels at the CpG sites cg05909553, cg19996418, cg17926016, cg18822414, cg08468965, cg01081091, and cg10248148 ( $P < 0.05$ ; [Supplementary Figure 1I](#)). Among the seven predicted CpG sites of *RECQL4*, cg19996418 was significantly correlated with LGG prognosis ([Supplementary Figure 1J](#) and [Supplementary Table 1](#)). Patients with low *RECQL4* methylation at the CpG site (cg19996418) had better overall survival than those with high *RECQL4* methylation levels ([Supplementary Figure 1J](#)).

## Interaction Network and Function of *BLM*, *RECQL4*, and Their ANGs in OS

The alteration frequencies for *BLM* and *RECQL4* ANGs were  $\geq 57.14\%$  and  $\geq 54.55\%$ , respectively, among the 50 most frequent ANGs in patients with OS ([Supplementary Tables 2](#) and [3](#)). *CRTC3* (71.43%), *CRTC3-AS1* (71.43%), and *HSPE1P3* (71.43%) were the most frequent ANGs of *BLM* in patients with OS ([Supplementary Table 2](#)). The most frequent ANGs for *RECQL4* in patients with OS were *ADCK5* (54.55%), *ARHGAP39* (54.55%), and *C8ORF82* (54.55%) ([Supplementary Table 3](#)). Twenty nodes and thirty-eight edges were identified in the PPI networks of *BLM* and its ANGs ([Figure 2A](#)). A complex interaction network was discovered between *BLM* and ANGs based on co-expression, physical interactions, shared protein domains, and colocalization ([Figure 2B](#)). Among *BLM* and its ANGs, *ARPIN-AP3S2*, *ARPIN*, *AP3S2*, *SLCO3A1*, and *RGMA* were identified as core genes ([Figure 2C](#)). Moreover, we obtained 42 nodes and 790 edges in the PPI networks of *RECQL4* and its ANGs ([Figure 2D](#)) and an intricate network of interactions between *RECQL4* and its ANGs, including co-expression, physical interactions, and colocalization ([Figure 2E](#)). Among *RECQL4* and its associated ANGs, *ADCK5*, *GPAAL1*, *CPSF1*, *LRRIC14*, and *EXOSC4* were identified as core genes ([Figure 2F](#)). Next, we analyzed the functions of *BLM*, *RECQL4*, and their ANGs in OS. The molecular functions of *BLM* and ANGs were mainly associated with enzyme inhibitor activity and phospholipid binding ([Figure 2G](#)). Furthermore, the regulation of protein phosphorylation, negative regulation of cell projection organization, cellular response to growth factor stimuli, cellular response to organic cyclic compounds, and endomembrane system organization were the main biological processes associated with *BLM* and its ANGs ([Figure 2H](#)). The cellular components of *BLM* and ANGs included the apical plasma membrane and microtubules ([Figure 2I](#)). Axonal guidance was the primary KEGG pathway associated with *BLM* and its ANGs ([Figure 2J](#)). The molecular functions of *RECQL4* and its ANGs were primarily associated with serine/threonine kinase activity and DNA-binding transcription factor-binding activity ([Figure 2K](#)). The regulation of DNA-binding transcription factor activity, response to peptide hormones, protein localization to organelles, and positive regulation of cellular component biogenesis were the main biological processes associated with *RECQL4* and its ANGs ([Figure 2L](#)).

## MiRNA and Kinase Targets of *BLM* and *RECQL4* in OS

The miRNA targets of *BLM* and *RECQL4* were identified using LinkedOmics software ([Supplementary Table 4](#)). miR-127, miR-516-5p, miR-141, and miR-200A were the miRNA targets of *BLM* in OS ( $P < 0.001$ ) ([Supplementary Table 4](#)). However, the miRNA targets of *RECQL4* in OS were miR-19B, miR-381, and miR-142-5p ( $P < 0.001$ ) ([Supplementary Table 4](#)). We identified the kinase targets of *BLM* and *RECQL4* in OS using LinkedOmics ([Supplementary Table 5](#)). Polo-like kinase 1 (PLK1), cyclin-dependent kinase 1 (CDK1), and Aurora kinase B (AURKB) were the kinase targets of *BLM* in patients with OS ( $P < 0.001$ ) ([Supplementary Table 5](#)). However, the kinase targets of *RECQL4* in OS were CDK1, PLK1, and cyclin-dependent kinase 2 (CDK2) ( $P < 0.001$ ) ([Supplementary Table 5](#)).

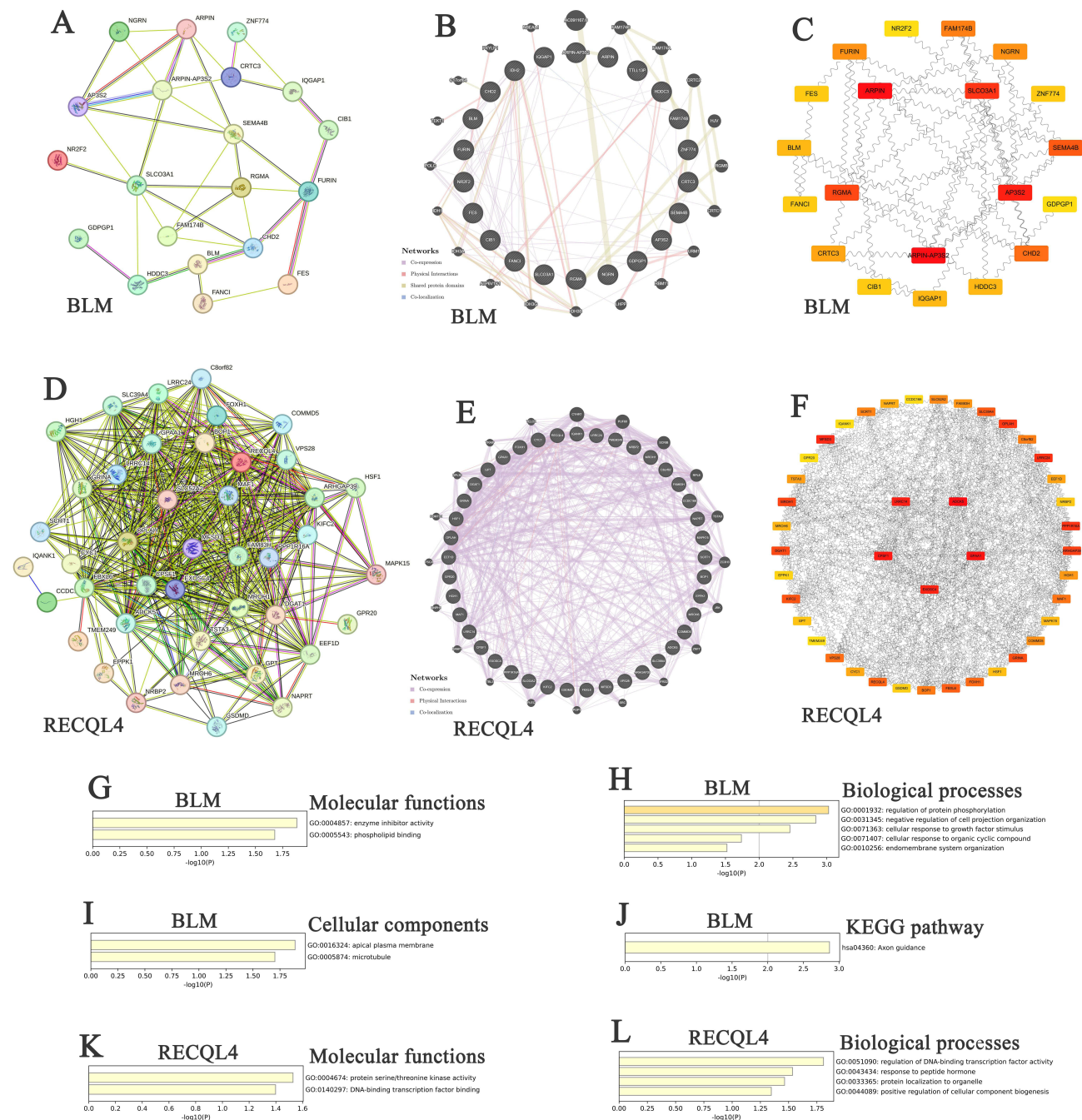


**Figure 2** Interaction and functional analyses of *BLM*, *RECQL4*, and their ANGs in OS. (**A** and **D**) PPI network of *BLM*, *RECQL4*, and their ANGs in OS, respectively (STRING); (**B** and **E**) Network analyses of *BLM*, *RECQL4*, and their ANGs in OS, respectively (GeneMANIA); (**C** and **F**) Core genes of *BLM*, *RECQL4*, and their ANGs in OS, respectively (Cytoscape); (**G** and **K**) Molecular functions of *BLM*, *RECQL4*, and their ANGs in OS, respectively (Metascape); (**H** and **L**) Biological processes of *BLM*, *RECQL4*, and their ANGs in OS, respectively (Metascape); (**I**) Cellular components of *BLM* and its ANGs in OS (Metascape); (**J**) KEGG of *BLM* and its ANGs in OS (Metascape).

## Correlation of Differentially Expressed Genes and *BLM* and *RECQL4* Expression in Patients with OS

A total of 8108 and 8740 genes were closely related to *BLM* and *RECQL4*, respectively, in patients with OS (Supplementary Figure 2A and B) (Supplementary Tables 6 and 7). Among them, 4628 and 4471 genes showed positive correlations and 3480 and 4269 genes showed negative correlations with *BLM* and *RECQL4* expression, respectively (Supplementary Figure 2A and B). Fifty genes showed significant positive or negative correlations with *BLM* and

*RECQL4* expression in patients with OS ([Supplementary Figure 2C–F](#)). *BLM* expression was strongly and positively correlated with *NCAPH* (Pearson's correlation coefficient [PCC] = 0.8248,  $P = 1.424e-65$ ; [Supplementary Figure 2G](#)), *C15orf42* (PCC = 0.8095,  $P = 2.291e-61$ ; [Supplementary Figure 2H](#)), and *CCNB2* (PCC = 0.8024,  $P = 1.537e-59$ ; [Supplementary Figure 2I](#)). The expression of *RECQL4* was positively correlated with *NFKBIL2* (PCC = 0.8162,  $P = 3.678e-63$ ; [Supplementary Figure 2J](#)), *TRAIIP* (PCC = 0.7505,  $P = 3.941e-48$ ; [Supplementary Figure 2K](#)), and *C16orf59* (PCC = 0.7301,  $P = 2.188e-44$ ; [Supplementary Figure 2L](#)).

## Correlation of Immune Cell Infiltration and *BLM* and *RECQL4* Expression and Anti-PD-1/CTLA-4/PD-L1 Immunotherapy in OS

*BLM* expression levels in patients with OS were negatively associated with immune cell infiltration (B cells, macrophages, and dendritic cells) ( $P < 0.05$ ; [Figure 3A](#)). Similarly, the expression levels of *RECQL4* in patients with OS were negatively associated with immune cell infiltration (CD8<sup>+</sup> T-cells, macrophages, and dendritic cells) ( $P < 0.05$ ; [Figure 3B](#)). Moreover, *BLM* and *RECQL4* expression in patients with OS was negatively correlated with the immune score ( $P < 0.05$ ; [Figure 3C–M](#)). *BLM* expression was significantly downregulated in patients with OS treated with anti-PD-1/PD-L1 ( $P = 0.05$ ) ([Figure 3N](#)). Similarly, *RECQL4* expression in patients with OS treated with anti-PD-1/CTLA-4, anti-PD-1/PD-L1, and anti-PD-1 antibodies were significantly downregulated ( $P = 0.05$ ) ([Figure 3O–Q](#)).

## Identify *BLM*<sup>+</sup> and *RECQL4*<sup>+</sup> Cells in OS Tissues

Given the prognostic value and unusual distribution of *BLM* and *RECQL4* in OS tissues, we aimed to explore the cell types in which they were enriched based on scRNA-seq data ([Supplementary Tables 8](#)). Analysis of the scRNA-seq data in the OS\_GSE162454 dataset identified 28 cell clusters and 8 cell types in OS tissues ([Figure 4A–C](#)). Monocytes/macrophage ( $n = 16682$ ) and malignant OS cells ( $n = 9443$ ) exhibited the highest cell counts ([Figure 4B and C](#)). *BLM* and *RECQL4* were significantly enriched in malignancies, particularly in the C13 cluster ([Figure 4D–G](#)). Cell–cell interaction (CCI) analysis revealed that *BLM*<sup>+</sup> and *RECQL4*<sup>+</sup> malignant OS cells mainly interacted with mono/macrophages and CD8Tex cells ([Figure 4H](#)).

## Therapeutic Drugs of *BLM* and *RECQL4* in OS

We used the BEST database to evaluate *BLM* and *RECQL4* low expression, which indicated drug resistance, and found that sphingosine kinase 1 inhibitor II and pilaralisib were the best drugs ([Figure 5A and B](#)). The Genomics of Drug Sensitivity in Cancer database was used to evaluate the inhibitory effects of *BLM* and *RECQL4* expression in OS cell lines. Sphingosine kinase 1 inhibitor II inhibited 919 cell lines with area under the curve (AUC) values  $> 0.928$  ([Figure 5C](#)). It exhibited good inhibitory effects on these cell lines ( $3.29 \leq IC_{50} (\mu M) \leq 187$ ) ([Figure 5D](#)). Furthermore, sphingosine kinase 1 inhibitor II had a high inhibitory effect on the 10 OS cell lines ( $0.9520 \leq AUC \leq 0.9782$ ,  $12.4443 \leq IC_{50} (\mu M) \leq 68.9717$ ) ([Figure 5E and F](#)). However, pilaralisib inhibited 919 cell lines with AUC values  $> 0.374$  ([Figure 5G](#)). It exhibited good inhibitory effects on these cell lines ( $0.573 \leq IC_{50} (\mu M) \leq 740$ ) ([Figure 5H](#)). Moreover, pilaralisib had a good inhibitory effect on the 10 OS cell lines ( $0.6988 \leq AUC \leq 0.9447$ ,  $5.3402 \leq IC_{50} (\mu M) \leq 138.5904$ ) ([Figure 5I and J](#)).

## Sphingosine Kinase I Inhibitor II and Pilaralisib Inhibit the Proliferation, Migration, and Invasion of 143B

As shown in [Figure 6A and B](#), the Cell Counting Kit-8 assay demonstrated that sphingosine kinase 1 inhibitor II (5, 10, 20, 40, 80, 160, and 320  $\mu M$ ) and pilaralisib significantly inhibited the proliferation of 143B cells ( $P < 0.01$ ). Furthermore, the wound-healing assay illustrated that 143B cells treated with sphingosine kinase 1 inhibitor II (40  $\mu M$ ) and pilaralisib (50  $\mu M$ ) displayed decreased migration capacity compared to the control cells ([Figure 6C and D](#);  $P < 0.01$ ). The results of the invasion assays showed that the number of migrating and invading cells decreased in 143B cells treated with sphingosine kinase 1 inhibitor II at a concentration of 40  $\mu M$  and pilaralisib at 50  $\mu M$  ([Figure 6E and F](#)) ( $P < 0.01$ ).

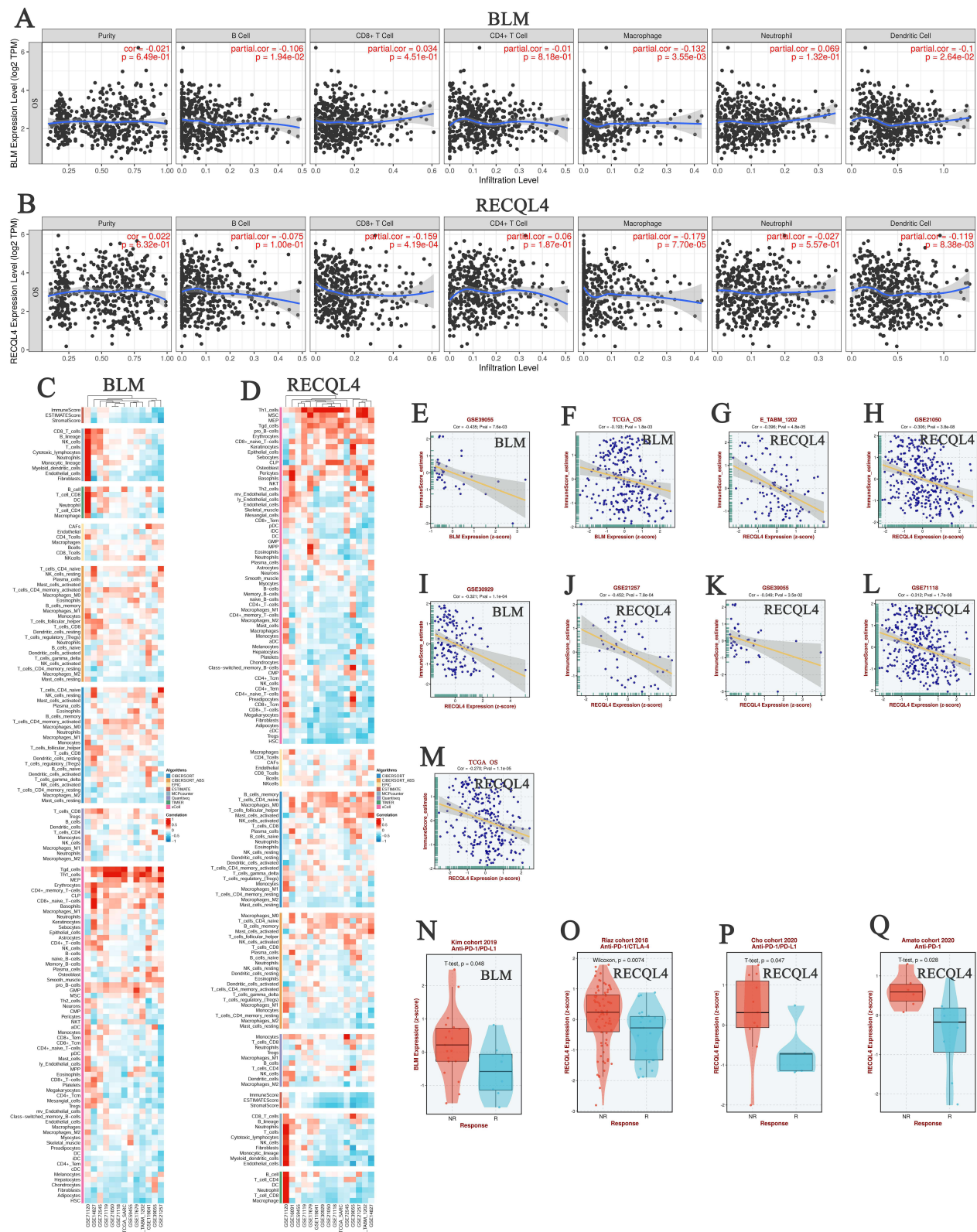


**Figure 3** Correlation between *BLM* and *RECQL4* expression, immune cell infiltration, and anti-PD-1/CTLA-4/4PD-L1 immunotherapy in OS. (**A** and **B**) Correlation between *BLM* and *RECQL4* expression and immune cell infiltration levels in OS, respectively (TIMER). (**C** and **D**) Heat maps showing the correlation between *BLM* and *RECQL4* and immune cell infiltration in OS, respectively (BEST). (**E** and **F**) Correlation between *BLM* expression and immune score in OS (BEST). (**G**–**M**) Correlation between *RECQL4* expression and immune score in OS (BEST). (**N**) Correlation between *BLM* expression and anti-PD-1/PD-L1 immunotherapy in OS (BEST). (**O**–**Q**) Correlation between *RECQL4* expression and anti-PD-1/CTLA-4/PD-L1 immunotherapy in OS (BEST).

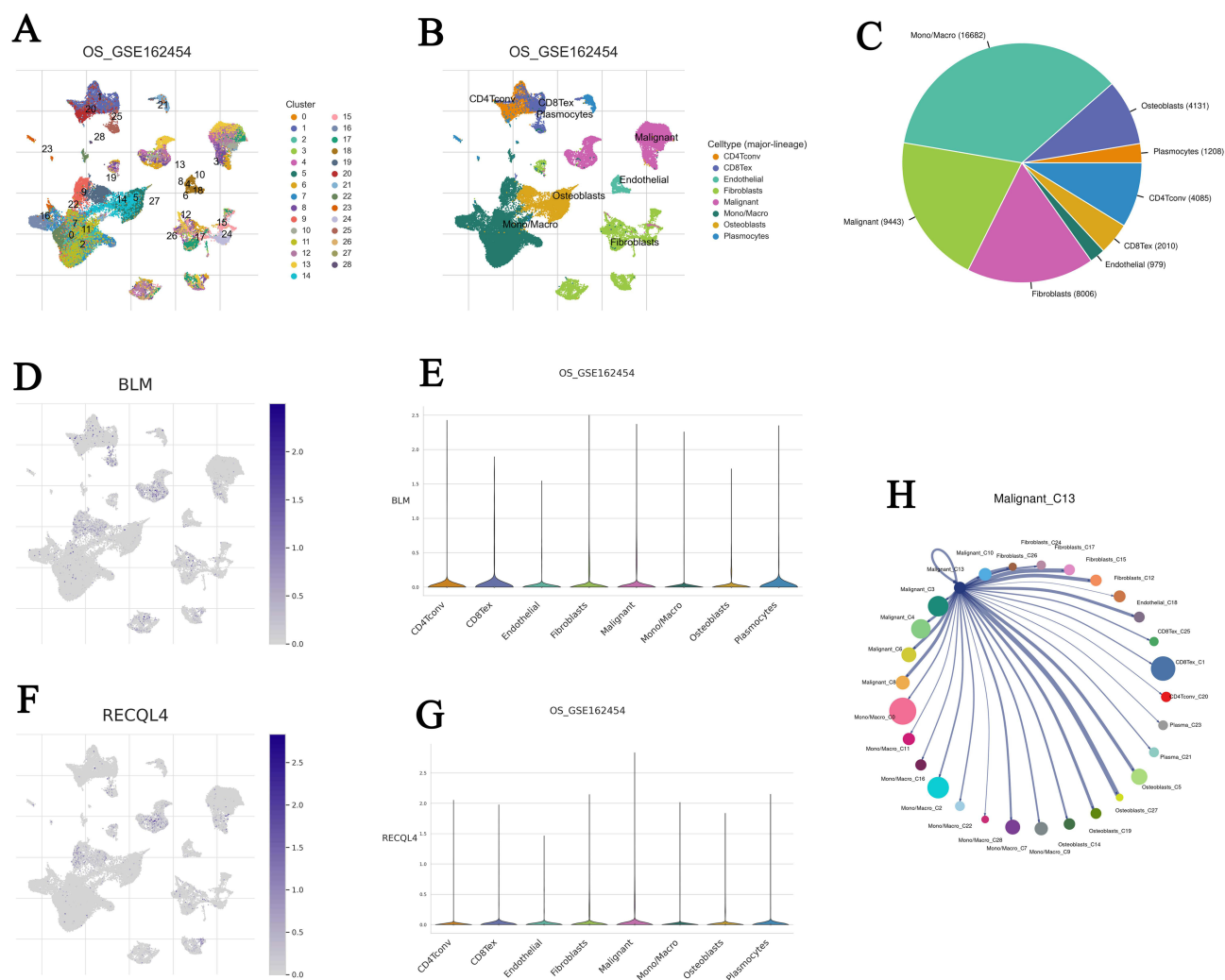


**Figure 4** *BLM* and *RECQL4* related cell-type distribution using the scRNA-seq database. **(A and B)** Identified *BLM* and *RECQL4* related cell clusters in OS tissues based on the GSE162454 dataset, respectively; **(C–G)** Distribution of *BLM* and *RECQL4* in different cells in GSE162454 dataset, respectively; **(H)** Interactions between *BLM*<sup>+</sup> and *RECQL4*<sup>+</sup> malignant C13 and other cells based on the GSE162454 dataset.

## Sphingosine Kinase I Inhibitor II and Pilaralisib Downregulate the Expression of *BLM* and *RECQL4* in 143B

Quantitative immunofluorescence was performed to determine differences in the expression of *BLM* and *RECQL4* in 143B cells treated with sphingosine kinase 1 inhibitor II and pilaralisib. Our results showed that both sphingosine kinase 1 inhibitor II and pilaralisib significantly inhibited the expression of *BLM* and *RECQL4* in 143B cells (Figure 7A–F) ( $P < 0.01$ ).

## *BLM* and *RECQL4* Silencing by siRNA Inhibits the Migration and Invasion of 143B

Western blotting showed that *BLM* and *RECQL4* protein expression levels in the *BLM* siRNA and *RECQL4* siRNA groups were significantly lower than those in the control siRNA group after transfection (Figure 8A–C) ( $P < 0.01$ ). Furthermore, wound-healing assays revealed that siRNA-mediated silencing of *BLM* and *RECQL4* significantly impaired the migratory capacity of 143B cells (Figure 8D and E) ( $P < 0.01$ ). Similarly, Transwell invasion assays showed a marked reduction in the number of invading 143B cells following *BLM*/*RECQL4* knockdown (Figure 8F and G) ( $P < 0.01$ ).

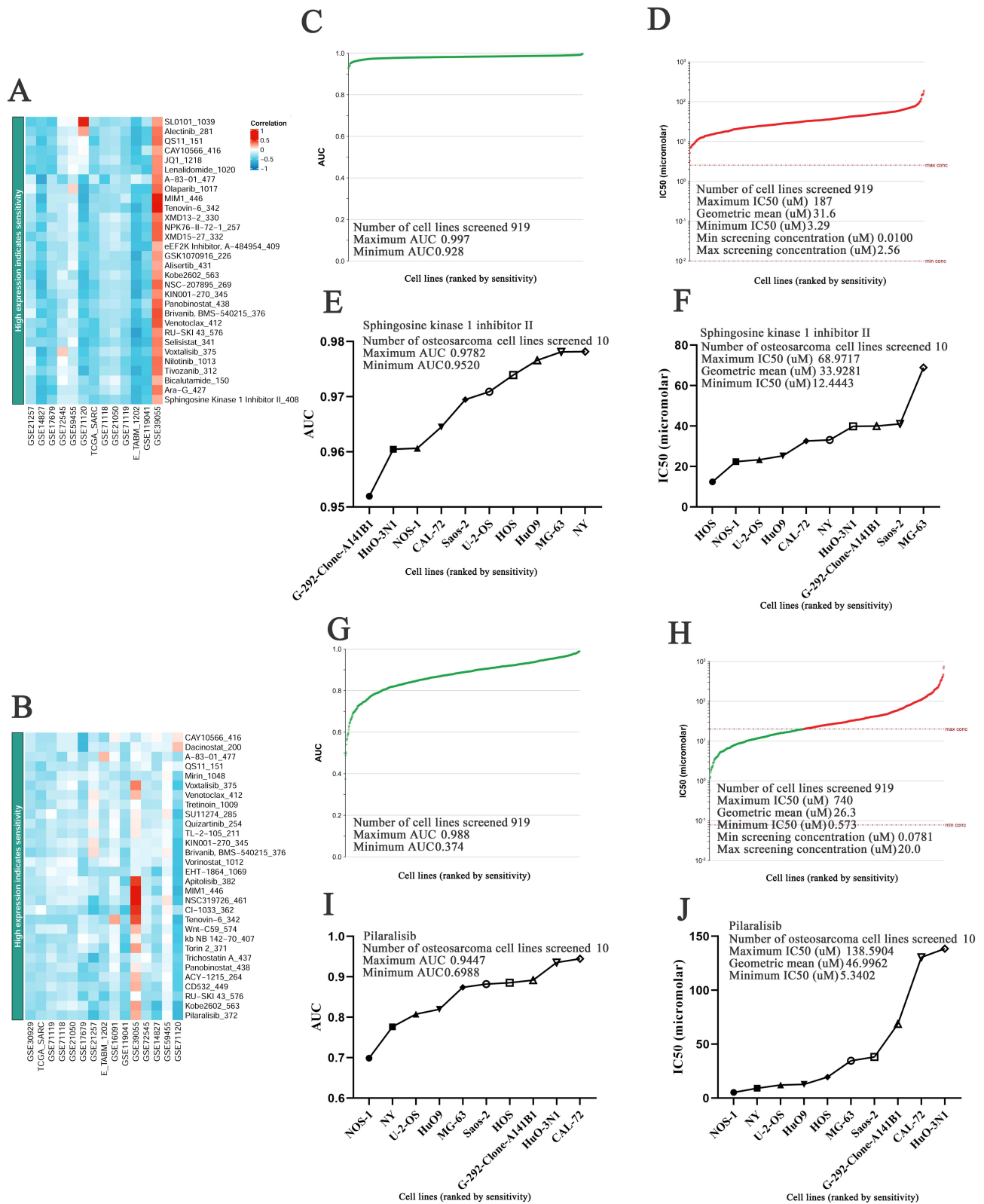


**Figure 5** IC<sub>50</sub> and AUC evaluation of sphingosine kinase I inhibitor II and pilaralisib in different cancer tissue types. **(A and B)** Heat maps showing *BLM* and *RECQL4* low expression indicate resistance drugs ranking, respectively (BEST); **(C and G)** AUC values of sphingosine kinase I inhibitor II and pilaralisib for the different cell lines, respectively (Genomics of drug sensitivity in cancer); **(D and H)** IC<sub>50</sub> values of sphingosine kinase I inhibitor II and pilaralisib for the different cell lines, respectively (Genomics of drug sensitivity in cancer); **(E and I)** AUC values of sphingosine kinase I inhibitor II and pilaralisib for OS cell line, respectively (Genomics of drug sensitivity in cancer); **(F and J)** IC<sub>50</sub> values of sphingosine kinase I inhibitor II and pilaralisib for OS cell line, respectively (Genomics of drug sensitivity in cancer).

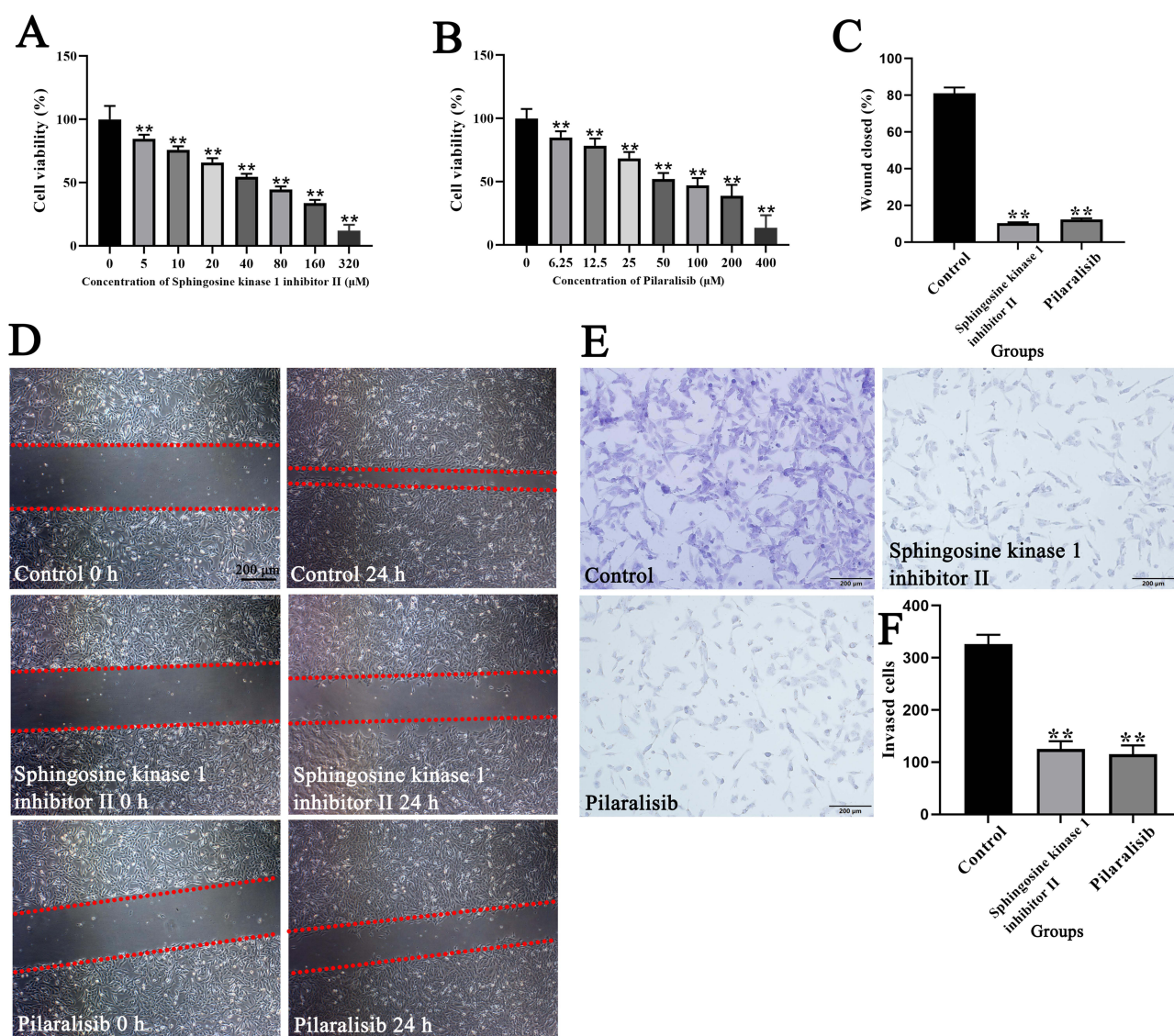


**Figure 6** Effects of sphingosine kinase 1 inhibitor II and pilaralisib on proliferation, migration, and invasion of 143B cells. Effect of sphingosine kinase 1 inhibitor II (**A**) and pilaralisib (**B**) at different concentrations on the proliferation of 143B cells; (**C** and **D**) Migration and repair abilities of 143B cells were compared using the wound-healing assay. The red dashed lines indicate the boundaries of the cell-free scratch wound; (**E** and **F**) Invasion abilities of 143B cells were compared using Transwell assays; Data are expressed as mean  $\pm$  SD of three replicates. \*\*  $P < 0.01$ , vs Control.

## Discussion

*BLM* and *RECQL4* mutations are associated with Bloom and Rothmund-Thomson syndromes, respectively. These syndromes not only exhibit overlapping clinical features but are also associated with an increased risk of cancer. Among these, patients with Rothmund-Thomson syndrome have the highest specific risk of OS.<sup>26</sup> This underscores the significant genetic influence on OS onset.<sup>31</sup> Although mutations in *BLM* and *RECQL4* have been confirmed to be associated with susceptibility to OS,<sup>32</sup> the expression patterns of these two genes in OS and their impact on the prognosis of patients with OS remain unknown. In this study, the transcriptional levels of *BLM* and *RECQL4* were significantly upregulated in patients with OS, suggesting their potential roles in promoting the occurrence and development of OS. Significant sex-related differences were observed in the transcription levels of *BLM* and *RECQL4*. Specifically, male patients exhibited significantly lower *BLM* transcriptional levels than female patients, whereas the opposite pattern was observed for *RECQL4*, with male patients exhibiting higher transcriptional levels. These sex disparities may be associated with sex hormone levels, genetic factors, or other unknown biological mechanisms, highlighting the

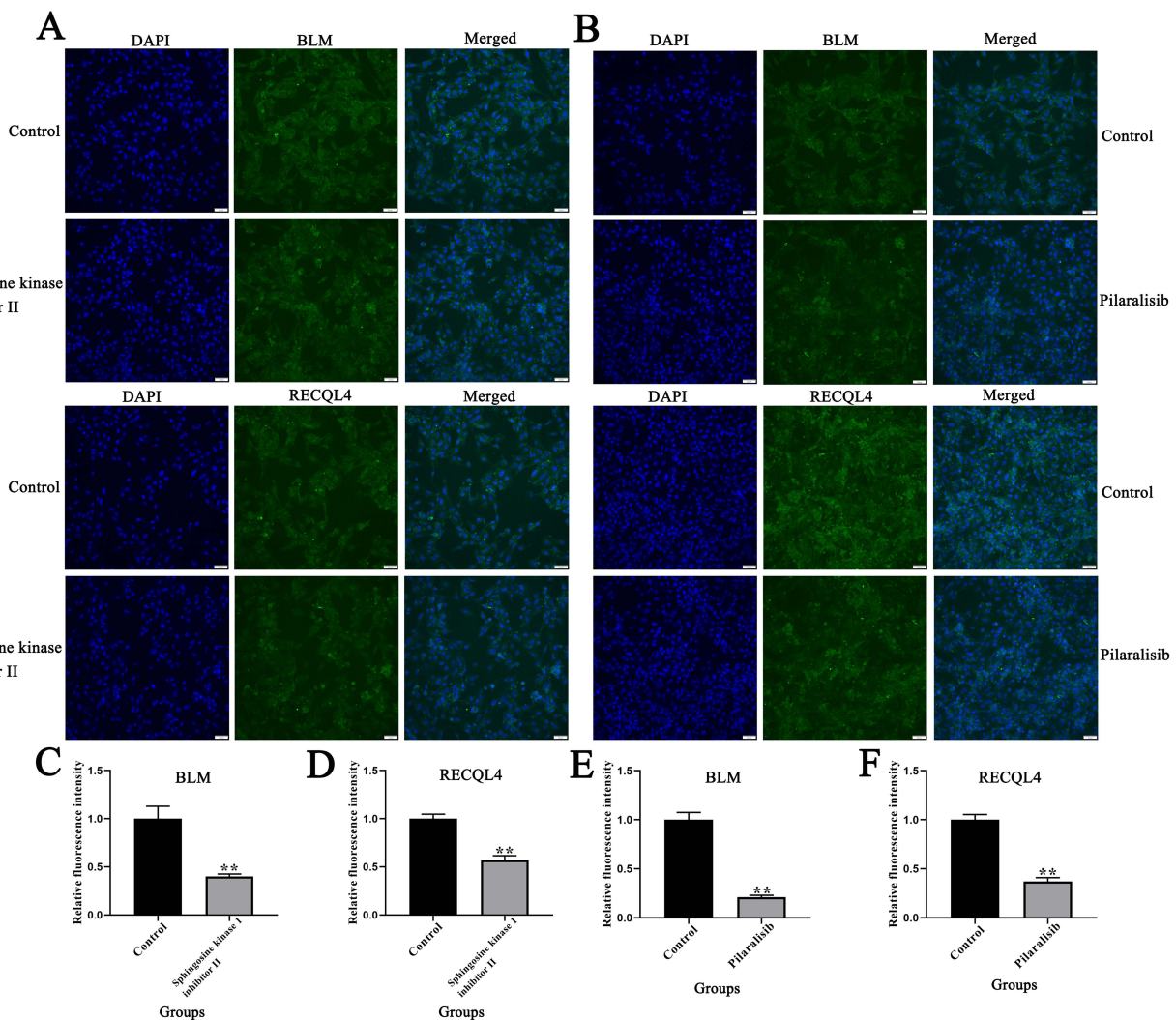


**Figure 7** Effects of sphingosine kinase I inhibitor II and pilaralisib on *BLM* and *RECQL4* expression in 143B cells. (**A** and **B**) Immunofluorescence analysis of the effects of sphingosine kinase I inhibitor II and pilaralisib on *BLM* and *RECQL4* expression in 143B cells. (**C–F**) Bar charts representing the effects of sphingosine kinase I inhibitor II and pilaralisib on *BLM* and *RECQL4* expression in 143B cells. Data are expressed as mean  $\pm$  SD of three replicates. \*\*  $P < 0.01$ , vs Control.

importance of considering sex factors in future studies on OS pathogenesis. In addition, the expression levels of *BLM* and *RECQL4* were closely correlated with the prognosis of patients with OS. Patients with low expression of *BLM* or *RECQL4* had longer overall and disease-free survival, indicating these two genes could serve as potential prognostic biomarkers to assist clinicians in evaluating patient prognosis and formulating personalized treatment plans.

To analyze the potential mechanisms underlying the abnormal expression of *BLM* and *RECQL4* in patients with OS, we systematically examined the mutation characteristics and methylation patterns of these two genes using the cBioPortal and MethSurv databases. Cancer progression is believed to be driven by the accumulation of genetic alterations and changes in gene expression patterns.<sup>33</sup> Genetic alterations occurred in 9% of *BLM* and 7% of *RECQL4* in patients with OS, primarily involving gene amplification and increased or decreased RNA levels. DNA methylation, a key chemical modification mechanism, plays an important role in determining cell type and lineage differentiation by regulating gene expression and genomic stability. Disruption of this regulatory network can induce various diseases, including cancer. A typical feature of cancer cells is an abnormal DNA methylation pattern, with targets mainly concentrated in the CpG island regions within the gene expression regulatory elements.<sup>34</sup> DNA methylation analysis showed that the methylation levels of multiple CpG sites in *BLM* and *RECQL4* changed significantly, and the methylation levels of some sites were significantly correlated with the prognosis of patients with OS. This indicates that DNA methylation may affect the

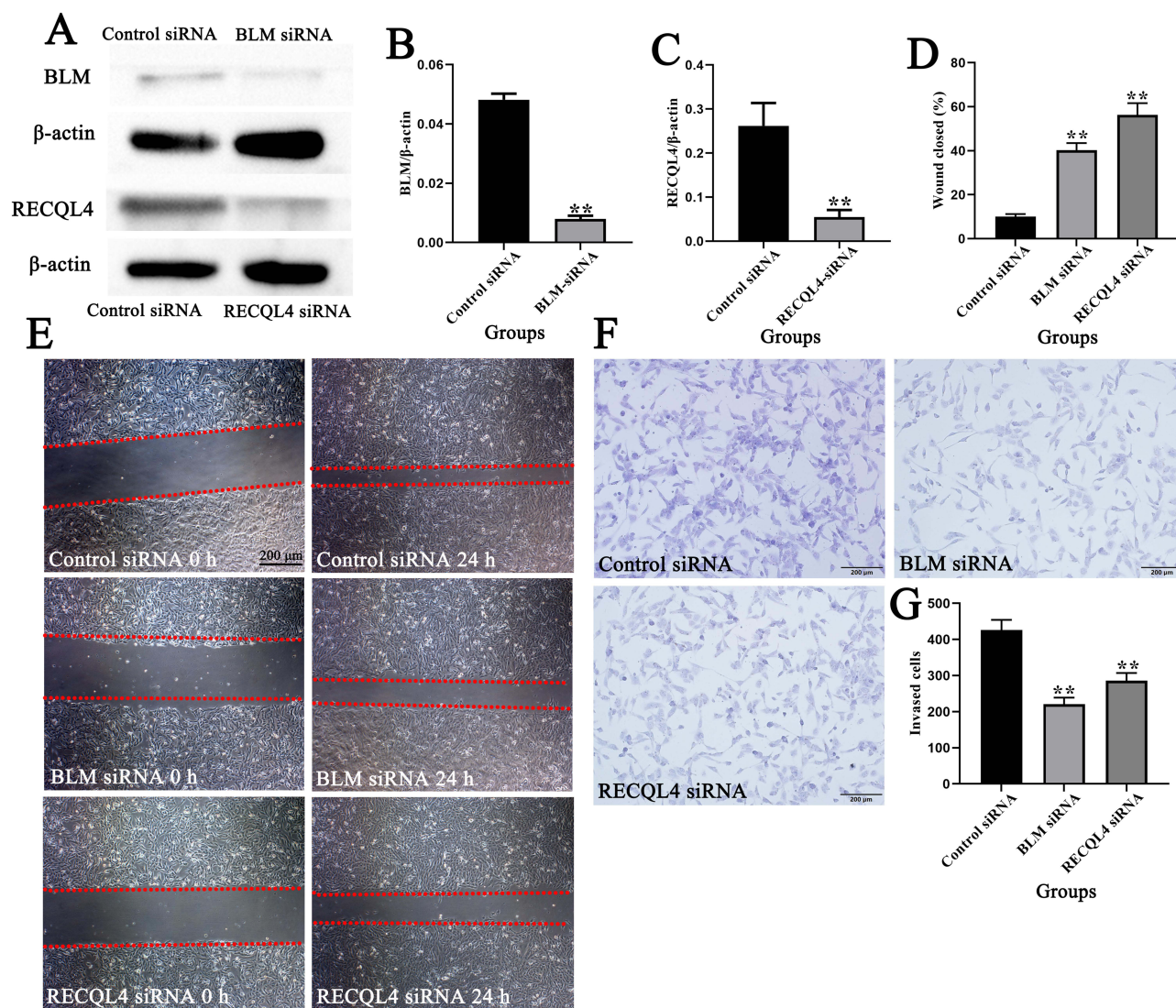


**Figure 8** *BLM* and *RECQL4* silencing by siRNA inhibited the migration and invasion of 143B cells; (**A–C**) Western blotting of *BLM* and *RECQL4* expression in 143B cells after siRNA silencing; (**D** and **E**) Migration and repair abilities of 143B cells after siRNA silencing were compared using a wound-healing assay. The red dashed lines indicate the boundaries of the cell-free scratch wound. (**F** and **G**) Invasion abilities of 143B cells after siRNA silencing were compared using Transwell assays. Data are expressed as mean  $\pm$  SD of three replicates. \*\*  $P < 0.01$ , vs Control.

occurrence and development of OS, as well as the prognosis of patients, by regulating *BLM* and *RECQL4* expression. As an important epigenetic regulatory mechanism, DNA methylation provides new targets and directions for epigenetic treatment of OS.

The occurrence and progression of cancer are often the result of the synergistic action of multiple gene abnormalities involving the accumulation of complex genetic alterations.<sup>35</sup> By constructing the interaction networks of *BLM*, *RECQL4*, and their ANGs, we identified multiple key interacting and core genes (including *ARPIN-AP3S2*, *ARPIN*, *ADCK5*, *GPAAI*) involved in various important molecular functions and biological processes. For example, *BLM* and its ANGs are primarily involved in enzyme inhibitor activity, phospholipid binding, and cellular responses to growth factor stimulation, whereas *RECQL4* and its ANGs are linked to protein serine/threonine kinase activity, DNA-binding transcription factor binding, and regulation of DNA-binding transcription factor activity. These functions predominantly influence tumor-related processes such as metabolism, proliferation, migration, and apoptosis.<sup>36,37</sup> These findings reveal the complex regulatory networks of *BLM* and *RECQL4* in OS, suggesting that these two genes may synergistically promote tumorigenesis and development by regulating several biological processes.

MicroRNAs (miRNAs) are a class of evolutionarily highly conserved small non-coding RNA molecules, approximately 22 nucleotides in length, which occupy a core position in the gene expression regulatory network.<sup>38</sup> Numerous studies have confirmed that dysregulation of miRNA expression is associated with abnormal alterations in genes related to cancer progression.<sup>39</sup> Kinases are a key class of enzymes that regulate cellular signaling pathways by catalyzing substrate protein phosphorylation. They are directly involved in the initiation, progression, and metastasis of cancer through functional abnormalities.<sup>40</sup> This study further identified the miRNA and kinase targets of *BLM* and *RECQL4* and found that these molecules (including miR-127, miR-19B, CDK1, and PLK1) can influence the malignant phenotypes of tumors, such as proliferation, migration, and invasion.<sup>41–44</sup> This suggests that they may inhibit the proliferation, migration, and invasion of OS cells by regulating *BLM* and *RECQL4* expression in patients with OS. These molecules are important therapeutic targets for regulating OS progression. In addition, we analyzed the correlation between the differentially expressed genes and *BLM* and *RECQL4* expression in patients with OS. The genes *NCAPH*, *C15orf42*, *CCNB2*, *NFKBIL2*, *TRAIIP*, and *C16orf59* were significantly positively correlated with *BLM* and *RECQL4* expression. These genes are associated with tumor progression,<sup>45,46</sup> suggesting that they may act as key regulatory genes in OS.

Immunotherapy has broad prospects for treating advanced cancers.<sup>47</sup> Several clinical trials have been conducted recently. Immunotherapy has received considerable attention because of its effectiveness in treating various tumors, and numerous preclinical experiments have supported its application in OS.<sup>48–50</sup> We found that the expression levels of *BLM* and *RECQL4* were negatively correlated with immune cell infiltration and immune scores. This indicates that these two genes may promote tumor immune escape by inhibiting the infiltration and function of immune cells, thereby creating an immunosuppressive tumor microenvironment. In addition, in patients who received anti-PD-1/CTLA-4/PD-L1 immunotherapy, the expression levels of *BLM* and *RECQL4* were significantly downregulated, suggesting that these genes may be associated with the immunotherapeutic response in OS. This discovery provides new ideas for using *BLM* and *RECQL4* as predictive markers of immunotherapy sensitivity and for exploring combination treatment strategies. Single-cell RNA sequencing revealed the cellular localization of *BLM* and *RECQL4* in OS tissues, showing their significant enrichment in malignant OS cells, particularly in the C13 cell cluster. Cell–cell interaction analysis revealed that *BLM*<sup>+</sup> and *RECQL4*<sup>+</sup> malignant OS cells primarily interacted with monocytes/macrophages and exhausted CD8<sup>+</sup> T-cells. This indicates that *BLM* and *RECQL4* may influence the immune status of the tumor microenvironment by regulating the interactions between tumor and immune cells, promoting tumor progression.

Sphingosine kinase 1 inhibitor II exerts multiple effects by inhibiting tumor proliferation and invasion and reversing the immunosuppressive microenvironment by targeting the abnormally activated SphK1/S1P pathway in tumor cells, demonstrating its potential as an antitumor drug.<sup>51</sup> As a phosphatidylinositol 3-kinase (PI3K) inhibitor, pilaralisib primarily exerts antitumor effects by inhibiting the PI3K pathway.<sup>52</sup> However, there have been no relevant reports on the roles of these two drugs in OS. Drug screening and functional experiments showed that sphingosine kinase 1 inhibitor II and pilaralisib had significant inhibitory effects on OS cells, suppressing the proliferation, migration, and invasion capabilities of 143B cells, while downregulating the expression levels of *BLM* and *RECQL4*. Further studies revealed that silencing *BLM* and *RECQL4* using siRNA significantly impaired the migration and invasion capabilities of the 143B cells. These results confirmed the key regulatory roles of *BLM* and *RECQL4* in the malignant biological behaviors of OS cells and revealed that sphingosine kinase 1 inhibitor II and pilaralisib may exert antitumor effects by targeting *BLM* and *RECQL4*, providing potential novel drugs and intervention targets for clinical OS treatment.

## Conclusion

In conclusion, this study systematically revealed the multiple mechanisms of action of *BLM* and *RECQL4* in OS, providing a new perspective for deepening our understanding of OS pathogenesis and laying the foundation for the development of *BLM* and *RECQL4*-based biomarkers and therapeutic strategies. However, this study had some limitations. For example, the relevant conclusions have not been validated in other OS cell lines and clinical samples, and the specific molecular mechanisms by which *BLM* and *RECQL4* regulate OS development have not been thoroughly explored. Further in-depth research is needed to promote the translation of these findings into clinical applications and to provide new therapeutic options for patients with OS.

## Abbreviations

OS, osteosarcoma; TISCH, Tumor Immune Single-cell Hub; PLK1, polo-like kinase 1; CDK1, cyclin-dependent kinase 1; AURKB, aurora kinase B; CCI, Cell–cell interaction; AUC, area under the curve.

## Data Sharing Statement

The datasets used and/or analyzed during the current study are available from the corresponding author (Hao Lin and Lijiao Peng) on reasonable request.

## Ethical Compliance Statement

All datasets utilized in this study were sourced from public databases, wherein all patient-related data had already obtained necessary ethical approvals, allowing free access for academic research and publication. Furthermore, this specific research project has received ethical approval from the Ethics Committee of the Affiliated Hospital of Guangdong Medical University (Approval No.: YJKT2025-298-01).

## Author Contributions

All authors made a significant contribution to the work reported, whether that is in the conception, study design, execution, acquisition of data, analysis and interpretation, or in all these areas; took part in drafting, revising or critically reviewing the article; gave final approval of the version to be published; have agreed on the journal to which the article has been submitted; and agree to be accountable for all aspects of the work.

## Funding

This research was funded by the Discipline Construction Project of Guangdong Medical University (4SG24001G) and the Natural Science Foundation of Guangdong Province, China (2025A1515011841).

## Disclosure

The authors report no conflicts of interest in this work.

## References

1. Siegel RL, Miller KD, Jemal A. *Cancer statistics*, 2018. *CA Cancer J Clin*. 2018;68(1):7–30. doi:10.3322/caac.21442
2. Sakamoto A, Iwamoto Y. Current status and perspectives regarding the treatment of osteo-sarcoma: chemotherapy. *Rev Recent Clin Trials*. 2008;3(3):228–231. doi:10.2174/157488708785700267
3. Anderson ME. Update on survival in osteosarcoma. *Orthop Clin North Am*. 2016;47(1):283–292. doi:10.1016/j.ocl.2015.08.022
4. Arndt CA, Rose PS, Folpe AL, Laack NN. Common musculoskeletal tumors of childhood and adolescence. *Mayo Clin Proc*. 2012;87(5):475–487. doi:10.1016/j.mayocp.2012.01.015
5. Berhe S, Danzer E, Meyers P, Behr G, LaQuaglia MP, Price AP. Unusual abdominal metastases in osteosarcoma. *J Pediatr Surg Case Rep*. 2018;28:13–16. doi:10.1016/j.epsc.2017.09.022
6. Bacci G, Rocca M, Salone M, et al. High grade osteosarcoma of the extremities with lung metastases at presentation: treatment with neoadjuvant chemotherapy and simultaneous resection of primary and metastatic lesions. *J Surg Oncol*. 2008;98(6):415–420. doi:10.1002/jso.21140
7. Sayles LC, Breese MR, Koehne AL, et al. Genome-informed targeted therapy for osteosarcoma. *Cancer Discov*. 2019;9(1):46–63. doi:10.1158/2159-8290.CD-17-1152
8. Yoshida A. Osteosarcoma: old and new challenges. *Surg Pathol Clin*. 2021;14(4):567–583. doi:10.1016/j.path.2021.06.003
9. Yu S, Yao X. Advances on immunotherapy for osteosarcoma. *Mol Cancer*. 2024;23(1):192. doi:10.1186/s12943-024-02105-9
10. Duffaud F, Mir O, Boudou-Rouquette P, et al. Efficacy and safety of regorafenib in adult patients with metastatic osteosarcoma: a non-comparative, randomised, double-blind, placebo-controlled, Phase 2 study. *Lancet Oncol*. 2019;20(1):120–133. doi:10.1016/S1470-2045(18)30742-3
11. Alfranca A, Martinez-Cruzado L, Tornin J, et al. Bone microenvironment signals in osteosarcoma development. *Cell Mol Life Sci*. 2015;72(16):3097–3113. doi:10.1007/s00018-015-1918-y
12. Brown HK, Tellez-Gabriel M, Heymann D. Cancer stem cells in osteosarcoma. *Cancer Lett*. 2017;386:189–195. doi:10.1016/j.canlet.2016.11.019
13. Köks G, Uudelepp ML, Limbach M, Peterson P, Reimann E, Köks S. Smoking-induced expression of the GPR15 gene indicates its potential role in chronic inflammatory pathologies. *Am J Pathol*. 2015;185(11):2898–2906. doi:10.1016/j.ajpath.2015.07.006
14. Kingo K, Mössner R, Köks S, et al. Association analysis of IL19, IL20 and IL24 genes in palmoplantar pustulosis. *Br J Dermatol*. 2007;156(4):646–652. doi:10.1111/j.1365-2133.2006.07731.x
15. Köks S, Männistö PT, Bourin M, Shlik J, Vasar V, Vasar E. Cholecystokinin-induced anxiety in rats: relevance of pre-experimental stress and seasonal variations. *J Psychiatry Neurosci*. 2000;25(1):33–42.

16. Poudel BH, Koks S. The whole transcriptome analysis using FFPE and fresh tissue samples identifies the molecular fingerprint of osteosarcoma. *Exp Biol Med.* 2024;249:10161. doi:10.3389/ebm.2024.10161
17. Ho XD, Nguyen HG, Trinh LH, et al. Analysis of the expression of repetitive DNA elements in osteosarcoma. *Front Genet.* 2017;8:193. doi:10.3389/fgene.2017.00193
18. Ho XD, Phung P, Q Le V. Whole transcriptome analysis identifies differentially regulated networks between osteosarcoma and normal bone samples. *Exp Biol Med.* 2017;242(18):1802–1811. doi:10.1177/1535370217736512
19. Reimann E, Köks S, Ho XD, Maasalu K, Märtson A. Whole exome sequencing of a single osteosarcoma case—integrative analysis with whole transcriptome RNA-seq data. *Hum Genomics.* 2014;8(1):20. doi:10.1186/s40246-014-0020-0
20. Larsen NB, Hickson ID. RecQ helicases: conserved guardians of genomic integrity. *Adv Exp Med Biol.* 2013;767:161–184.
21. Rezazadeh S. RecQ helicases; at the crossroad of genome replication, repair, and recombination. *Mol Biol Rep.* 2012;39(4):4527–4543. doi:10.1007/s11033-011-1243-y
22. Zhu X, Chen H, Yang Y, et al. Distinct prognosis of mRNA expression of the five RecQ DNA-helicase family members - RECQL, BLM, WRN, RECQL4, and RECQL5 - in patients with breast cancer. *Cancer Manag Res.* 2018;10:6649–6668. doi:10.2147/CMAR.S185769
23. Arora A, Abdel-Fatah TM, Agarwal D, et al. Transcriptomic and protein expression analysis reveals clinicopathological significance of bloom syndrome helicase (BLM) in breast cancer. *Mol Cancer Ther.* 2015;14(4):1057–1065. doi:10.1158/1535-7163.MCT-14-0939
24. Zhao M, Chen Z, Zheng Y, et al. Identification of cancer stem cell-related biomarkers in lung adenocarcinoma by stemness index and weighted correlation network analysis. *J Cancer Res Clin Oncol.* 2020;146(6):1463–1472. doi:10.1007/s00432-020-03194-x
25. Qian X, Feng S, Xie D, Feng D, Jiang Y, Zhang X. RecQ helicase BLM regulates prostate cancer cell proliferation and apoptosis. *Oncol Lett.* 2017;14(4):4206–4212. doi:10.3892/ol.2017.6704
26. Wang LL, Gannavarapu A, Kozinetz CA, et al. Association between osteosarcoma and deleterious mutations in the RECQL4 gene in Rothmund-Thomson syndrome. *J Natl Cancer Inst.* 2003;95(9):669–674. doi:10.1093/jnci/95.9.669
27. Viziteu E, Kassambara A, Pasero P, Klein B, Moreaux J. RECQ helicases are deregulated in hematological malignancies in association with a prognostic value. *Biomark Res.* 2016;4:3. doi:10.1186/s40364-016-0057-4
28. Situ Y, Deng L, Huang Z, et al. CDH2 and CDH13 as potential prognostic and therapeutic targets for adrenocortical carcinoma. *Cancer Biol Ther.* 2024;25(1):2428469. doi:10.1080/15384047.2024.2428469
29. Shao Z, Lu L, Cui Y, et al. PYCR in kidney renal papillary cell carcinoma: expression, prognosis, gene regulation network, and regulation targets. *Front Biosci.* 2022;27(12):336. doi:10.31083/j.fbl2712336
30. Sun D, Wang J, Han Y, et al. TISCH: a comprehensive web resource enabling interactive single-cell transcriptome visualization of tumor microenvironment. *Nucleic Acids Res.* 2021;49(D1):D1420–D1430. doi:10.1093/nar/gkaa1020
31. Lill CM, Hansen J, Olsen JH, Binder H, Ritz B, Bertram L. Impact of Parkinson's disease risk loci on age at onset. *Mov Disord.* 2015;30(6):847–850. doi:10.1002/mds.26237
32. Lu L, Jin W, Wang LL. RECQ DNA Helicases and Osteosarcoma. *Adv Exp Med Biol.* 2020;1258:37–54.
33. Garnis C, Buys TP, Lam WL. Genetic alteration and gene expression modulation during cancer progression. *Mol Cancer.* 2004;3:9. doi:10.1186/1476-4598-3-9
34. Nishiyama A, Nakanishi M. Navigating the DNA methylation landscape of cancer. *Trends Genet.* 2021;37(11):1012–1027. doi:10.1016/j.tig.2021.05.002
35. Takeshima H, Ushijima T. Accumulation of genetic and epigenetic alterations in normal cells and cancer risk. *NPJ Precis Oncol.* 2019;3:7. doi:10.1038/s41698-019-0079-0
36. Stoica C, Ferreira AK, Hannan K, Bakovic M. Bilayer forming phospholipids as targets for cancer therapy. *Int J Mol Sci.* 2022;23(9):5266. doi:10.3390/ijms23095266
37. Bushweller JH. Targeting transcription factors in cancer - from undruggable to reality. *Nat Rev Cancer.* 2019;19(11):611–624. doi:10.1038/s41568-019-0196-7
38. Bartel DP. Metazoan MicroRNAs. *Cell.* 2018;173(1):20–51. doi:10.1016/j.cell.2018.03.006
39. He B, Zhao Z, Cai Q, et al. miRNA-based biomarkers, therapies, and resistance in Cancer. *Int J Biol Sci.* 2020;16(14):2628–2647. doi:10.7150/ijbs.47203
40. DeRyckere D, Huelse JM, Earp HS, Graham DK. TAM family kinases as therapeutic targets at the interface of cancer and immunity. *Nat Rev Clin Oncol.* 2023;20(11):755–779. doi:10.1038/s41571-023-00813-7
41. Sheng S, Hu Y, Yu F, et al. circKIF4A sponges miR-127 to promote ovarian cancer progression. *Aging.* 2020;12(18):17921–17929. doi:10.18632/aging.103389
42. Song M, Sun M, Xia L, et al. miR-19b-3p promotes human pancreatic cancer Capan-2 cells proliferation by targeting phosphatase and tension homolog. *Ann Transl Med.* 2019;7(11):236. doi:10.21037/atm.2019.04.61
43. Yasukawa M, Ando Y, Yamashita T, et al. CDK1 dependent phosphorylation of hTERT contributes to cancer progression. *Nat Commun.* 2020;11(1):1557. doi:10.1038/s41467-020-15289-7
44. Iliaki S, Beyaert R, Afonina IS. Polo-like kinase 1 (PLK1) signaling in cancer and beyond. *Biochem Pharmacol.* 2021;193:114747. doi:10.1016/j.bcp.2021.114747
45. Liu C, Han X, Zhang S, et al. The role of NCAPH in cancer treatment. *Cell Signal.* 2024;121:111262. doi:10.1016/j.cellsig.2024.111262
46. Yu J, Li M, Ju L, et al. TRAIIP suppresses bladder cancer progression by catalyzing K48-linked polyubiquitination of MYC. *Oncogene.* 2024;43(7):470–483. doi:10.1038/s41388-023-02922-0
47. Baxevasis CN, Perez SA, Papamichail M. Cancer immunotherapy. *Crit Rev Clin Lab Sci.* 2009;46(4):167–189. doi:10.1080/10408360902937809
48. Wedekind MF, Wagner LM, Cripe TP. Immunotherapy for osteosarcoma: where do we go from here? *Pediatr Blood Cancer.* 2018;65(9):e27227. doi:10.1002/pbc.27227
49. Chen C, Xie L, Ren T, Huang Y, Xu J, Guo W. Immunotherapy for osteosarcoma: fundamental mechanism, rationale, and recent breakthroughs. *Cancer Lett.* 2021;500:1–10. doi:10.1016/j.canlet.2020.12.024
50. Hashimoto K, Nishimura S, Goto K. PD-1/PD-L1 immune checkpoint in bone and soft tissue tumors (Review). *Mol Clin Oncol.* 2025;22(4):31. doi:10.3892/mco.2025.2826

51. Yang YL, Ji C, Cheng L, et al. Sphingosine kinase-1 inhibition sensitizes curcumin-induced growth inhibition and apoptosis in ovarian cancer cells. *Cancer Sci.* 2012;103(8):1538–1545. doi:10.1111/j.1349-7006.2012.02335.x
52. Edelman G, Rodon J, Lager J, et al. Phase I trial of a tablet formulation of pilaralisib, a pan-class I PI3K inhibitor, in patients with advanced solid tumors. *Oncologist.* 2018;23(4):401–e38. doi:10.1634/theoncologist.2017-0691

**ImmunoTargets and Therapy**

**Dovepress**  
Taylor & Francis Group

### **Publish your work in this journal**

ImmunoTargets and Therapy is an international, peer-reviewed open access journal focusing on the immunological basis of diseases, potential targets for immune based therapy and treatment protocols employed to improve patient management. Basic immunology and physiology of the immune system in health, and disease will be also covered. In addition, the journal will focus on the impact of management programs and new therapeutic agents and protocols on patient perspectives such as quality of life, adherence and satisfaction. The manuscript management system is completely online and includes a very quick and fair peer-review system, which is all easy to use. Visit <http://www.dovepress.com/testimonials.php> to read real quotes from published authors.

Submit your manuscript here: <http://www.dovepress.com/immnotargets-and-therapy-journal>